Rap-Phr systems in *B. subtilis* 3610 affect matrix gene expression and play a role in biofilm formation in vitro and on the plant root

Mathilde Nordgaard Christensen[1], Rasmus Møller Rosenbek Mortensen[1], Nikolaj Kaae Kirk[1], Ramses Gallegos-Monterrosa[2] and Ákos T. Kovács[1]

[1] Bacterial Interactions and Evolution Group, DTU Bioengineering, Technical University of Denmark, 2800 Kongens Lyngby, Denmark

[2] Terrestrial Biofilms Group, Institute of Microbiology, Friedrich-Schiller-University Jena, 07743 Jena, Germany

For correspondence: E-mail: atkovacs@dtu.dk; Søltofts Plads Building 221, 2800 Kongens Lyngby, Denmark, Tel. +45 4525 2527; Fax: +45 4588 4922

Keywords: *Bacillus subtilis*, Rap-Phr, matrix gene expression, biofilm formation, root colonization

Summary

Natural isolates of the soil-dwelling bacterium *Bacillus subtilis* form robust biofilms under laboratory conditions and colonize plant roots. *B. subtilis* biofilm gene expression displays phenotypic heterogeneity that is influenced by a family of Rap-Phr regulatory systems. Most Rap-Phr systems have been studied independently, in different genetic backgrounds and under distinct conditions, hampering true comparison of the Rap-Phr systems' impact on bacterial differentiation. Here, we investigated each of the 12 Rap-Phr systems of *B. subtilis* NCIB 3610 for their role in biofilm formation. While 11 *Δrap-phr* mutants displayed increased matrix gene expression under biofilm inducing conditions, only some of the mutants demonstrated altered biofilm formation and colonization of *Arabidopsis thaliana* roots. Therefore, matrix gene expression does not directly correlate with biofilm formation *in vitro* and on the root. Our results suggest that each of the 12 Rap-Phr systems influences matrix gene expression, thereby allowing fine-tuning of the timing and level of matrix production in response to specific conditions, but additional factors also contribute to biofilm architecture and root colonization.

Significance Statement

Natural isolates of *Bacillus subtilis* form robust biofilms *in vitro* and on plant roots. The formation of these heterogeneous populations is regulated by diverse Rap-Phr systems. However, most Rap-Phr systems have been studied independently and in different genetic backgrounds. Here, we report that all 12 Rap-Phr systems affect matrix gene expression and demonstrate that matrix production does not directly correlate with biofilm formation and root colonization. Our study highlights the importance of the Rap-Phr systems in environmental adaptation of *B. subtilis*, specifically during biofilm formation in the rhizosphere.

Introduction

In nature, biofilms are the predominant lifestyle of bacteria and are known as surface-associated microbial communities embedded in a self-produced matrix (Hall-Stoodley *et al.*, 2004; Flemming and Wingender, 2010; López *et al.*, 2010). Biofilms have been widely studied since they represent a fascinating example of microbial development in response to environmental cues (O'Toole *et al.*, 2000). Furthermore, studying biofilms is of special interest due to their detrimental impact in clinical and industrial settings (Stewart, 2002; Di Pippo *et al.*, 2018) as well as their promising potential within the biotechnology industry (Singh *et al.*, 2006; Blake *et al.*, 2021). Regarding the latter, the Gram-positive bacterium *Bacillus subtilis* has in the last two decades gained increased interest due to its promising potential as a biocontrol agent within agriculture (Ongena and Jacques, 2008; Kiesewalter *et al.*, 2021). In its natural habitat, the soil-dwelling bacterium colonizes plants by forming a biofilm on the root (Bais *et al.*, 2004; Chen *et al.*, 2012; Beauregard *et al.*, 2013). After successfully colonizing the root, *B. subtilis* exerts its plant-beneficial properties, including directly promoting plant growth as well as protecting the plant against diseases (Blake *et al.,* 2021). Furthermore, *B. subtilis* forms spores that are highly resistant to extreme environments (Piggot and Hilbert, 2004) facilitating easy formulation and storage of *B. subtilis* for application within agriculture (Ongena and Jacques, 2008).

B. subtilis can easily be isolated from the rhizosphere of plants (Fall *et al.*, 2004), and a study performed by Chen *et al.* (2013) showed that the majority of natural strains isolated from rhizosphere soils formed architecturally complex biofilms under laboratory conditions, indicating that biofilm formation is an important trait for *B. subtilis* to thrive in its natural habitat. In the laboratory, *B. subtilis* has long been studied using different kinds of biofilm models including colonies at the air-agar interface as well as floating biofilms formed at the air-medium interface, termed pellicles (Arnaouteli *et al.*, 2021). The extensive repetitive cultivation of *B. subtilis* under laboratory conditions and mutagenesis has led to domestication of strains; for example, certain isolates of 168 form severely attenuated biofilms due to

mutations acquired under the domestication process (McLoon *et al.*, 2011), while other variants of the 168 strain still retained their ability to form robust pellicles in biofilm-inducing rich medium (Gallegos-Monterrosa *et al.*, 2016)). Importantly, the well-used undomesticated strain *B. subtilis* NCIB 3610 (hereafter 3610) forms architecturally complex colonies and robust, wrinkled pellicles (Branda *et al.*, 2001).

A prevalent feature of *B. subtilis* biofilms is that they display complex phenotypic heterogeneity, where genetically identical cells differentiate into distinct cell types in response to external cues (Lopez *et al.*, 2009; López and Kolter, 2010). The variation in environmental conditions throughout the biofilm (Costerton *et al.*, 1994) thereby leads to a heterogeneous population with different cell types performing distinct tasks and occupying different micro-niches. The external signals triggering cell differentiation include quorum-sensing molecules, natural products, and nutrient availability that activate a set of sensor kinases (Mhatre *et al.*, 2014; Arnaouteli *et al.*, 2021). Once activated, the sensor kinases phosphorylate their respective master transcriptional regulators, Spo0A, DegU and ComA, each of which activates different sets of genes (López and Kolter, 2010). The Spo0A pathway governs differentiation into matrix-producing cells as well as sporulating cells. In response to external cues, one or more of five histidine kinases, KinA-E, are activated which results in phosphorylation of Spo0F. Spo0F~P then transfers its phosphoryl group to Spo0B, which in turn transfers the phosphoryl group to and thereby activates Spo0A (Jiang *et al.*, 2000; Fujita *et al.*, 2005). At low Spo0A~P levels, the genes involved in the synthesis of matrix components, exopolysaccharide (EPS) and TasA protein fiber, are expressed (Fujita *et al.*, 2005; Cairns *et al.*, 2014). These two matrix components are well known to be required for biofilm formation *in vitro* and on the plant root (Branda *et al.*, 2006; Beauregard *et al.*, 2013). When high levels of Spo0A~P are reached, genes involves in sporulation are expressed (Fujita *et al.*, 2005). The DegU response regulator is phosphorylated by its cognate histidine kinase DegS. Studies have indicated that inhibition of flagellar rotation, as may take place upon contact with a surface, acts as a mechanical trigger to activate the DegS-

DegU two-component signaling pathway (Cairns *et al.*, 2013). At very low levels of DegU~P, genes related to swarming motility are expressed, while elevated levels of DegU~P induce exoprotease production and at the same time represses motility genes (Verhamme *et al.*, 2007; Belas, 2013). Finally, the pheromone ComX activates the histidine kinase ComP, which phosphorylates ComA, resulting in expression of genes involved in competence development and surfactin production (Comella and Grossman, 2005).

This regulatory network governing cell differentiation in *B. subtilis* is further regulated by a family of response regulator aspartyl-phosphate (Rap) phosphatases and their associated phosphatase regulator (Phr) peptides. In the *B. subtilis* group, 80 distinct putative *rap-phr* alleles have been identified with a strain having on average 11 *rap* genes (Even-Tov *et al.*, 2016). The genes encoding the Rap-Phr pairs are found as gene cassettes with the *phr* gene downstream of the *rap* gene and the expression of these being translationally coupled (Reizer *et al.*, 1997; Pottahil and Lazazzera, 2003). Some exceptions to this exist, for example the *rapB* gene is not followed by an active peptide encoding gene (Perego *et al.*, 1996). Moreover some Rap proteins are regulated by Phr peptides encoded in other cassettes, e.g. RapB and J are both controlled by PhrC (Parashar *et al.*, 2013). When expressed, the Rap phosphatases exert their effect within the cell by either dephosphorylating Spo0F~P (thus hindering Spo0A phosphorylation) or inhibiting the DNA binding activity of ComA or DegU (Perego, 2013). In contrast, the *phr* gene product follows another path; it is first secreted out of the cell through the Sec-dependent export pathway and processed into mature five to six amino acid signaling peptides. At high cell density, the Phr peptides reach threshold concentrations at which they are transported back into the cell by the oligopeptide permease (Opp). Once within the cell, the Phr peptides will inhibit their cognate Rap proteins, thereby relieving the inhibition of the master regulators resulting in altered gene expression (Pottahil and Lazazzera, 2003; Perego, 2013). The Rap-Phr systems thereby act as quorum sensing systems, allowing the bacteria to respond to environmental changes only at sufficient cell densities.

As expected by the diversity and abundance of multiple Rap-Phr systems regulating the activity of these three master regulators, the Rap phosphatases show high redundancy in their regulatory function: RapA, B, E, H, I, J and P have been shown to dephosphorylate Spo0F~P, RapC, D, F, H, K and P regulate ComA, while RapG has been shown to regulate the activity of DegU (Auchtung *et al.*, 2006; Ogura and Fujita, 2007; Perego, 2013; Omer Bendori *et al.*, 2015). However, this overall overview of the Rap-Phr signaling network is based on studies where most Rap-Phr systems have been tested independently from each other, in different genetic backgrounds and under distinct cultivation conditions (Perego, 2013). Additionally, previous investigations have directed their study towards certain targets of Rap-Phr regulation, with RapA and B being mostly studied for their impact on sporulation (Perego and Hoch, 1996), while RapC and F have been shown to be involved in competence development (Core and Perego, 2003; Bongiorni *et al.*, 2005). So far, only RapP has been demonstrated to impact biofilm formation (Parashar *et al.*, 2013; Omer Bendori *et al.*, 2015). We recently studied all 12 Rap-Phr systems of *B. subtilis* 3610 in the same genetic background by competing all single and double Δ*rap-phr* mutants as well the WT under different selective conditions. This study highlighted that the variability in Rap-Phr systems affected the ability to compete in diverse environments (Gallegos-Monterrosa *et al.*, 2020).

In this study, we investigated the impact of each of the 12 Rap-Phr systems in *B. subtilis* 3610 on biofilm formation. First, matrix gene expression of wild type (WT) and the 12 single Δ*rap-phr* mutants was analyzed under biofilm-inducing conditions. Next, we tested the mutants for the ability to form architecturally complex biofilms *in vitro*. Finally, the impact of each of the Rap-Phr systems on biofilm formation in a more ecologically relevant environment was investigated by testing the mutants for plant root colonization. We found that all 12 mutants showed altered matrix gene expression compared to the WT. In addition, in accordance with a previous study (Gallegos-Monterrosa *et al.*, 2016), we found that increased matrix gene expression did not necessarily manifest in more complex biofilms *in vitro* and on the root.

Results

*Single Δ*rap-phr *mutants show altered matrix gene expression compared to the WT*

To study the role of the Rap-Phr systems in biofilm formation, *B. subtilis* DK1042 strain (a natural competent derivative of the undomesticated NCBI 3610) (Konkol *et al.*, 2013) was used as WT. In contrast to domesticated strains which may have acquired mutations to the Rap-Phr systems or even lost some of them, NCIB 3610 and DK1042 contain all 12 *rap-phr* modules (McLoon *et al.*, 2011).

The diversity in Rap-Phr regulatory systems as well as the reported role of several of the Rap phosphatases in regulating the activity of Spo0A (Perego, 2013; Omer Bendori *et al.*, 2015), which controls matrix gene expression, prompted us to test the impact of each of the 12 Rap-Phr modules on matrix gene expression. For this purpose, WT and the 12 single Δ*rap-phr* mutants (Gallegos-Monterrosa *et al.*, 2020), each lacking one of the *rap-phr* modules, were labeled with a P_{tapA}-*gfp* reporter construct. To quantify matrix gene expression during biofilm formation, we used a previously established approach (Kearns et al. 2005). This method utilizes that expression from the promoters of the *tapA-sipW-tasA* operon, responsible for the production of the protein component of the extracellular matrix (Branda *et al.*, 2006). The expression of this operon is highly induced during late exponential growth phase under shaking conditions in MSgg, a medium known to induce biofilm formation. After 6h of growth in MSgg under shaking conditions, the fluorescence intensities of WT and mutants were measured using flow cytometry.

Since RapA, B, E, H, I, J and P have been reported to dephosphorylate Spo0F~P (Perego, 2013; Omer Bendori *et al.*, 2015), we hypothesized that the mutants lacking one of these Rap phosphatases would have a larger relative ON population (i.e. cells in the high expression state), due to more cells committing to matrix production, and/or display a higher mean expression from P_{tapA} in the ON population due to earlier matrix gene expression, as compared to the WT. Indeed, only *ΔrapA* showed a significantly smaller relative ON population ($p=0.022$, $n=3-8$) than the WT (Fig. 1). In contrast, all mutants except *ΔrapA* showed a significantly higher mean expression of the ON population compared to the WT. The increased mean

expression by the mutants could potentially be caused by enhanced growth in MSgg, as strains growing faster would reach the threshold density for biofilm formation earlier, and thus show increased matrix gene expression. However, when the optical density (OD) at 600 nm was measured after 6 h in MSgg prior to flow cytometry analysis, the mutants showed either similar or reduced OD_{600} compared to WT, thus excluding this explanation. Interestingly, the increased matrix gene expression was not limited to the mutants lacking one of the Rap phosphatases reported to dephosphorylate Spo0F~P activity. These results show that all 12 Rap-Phr regulatory systems influence matrix gene expression.

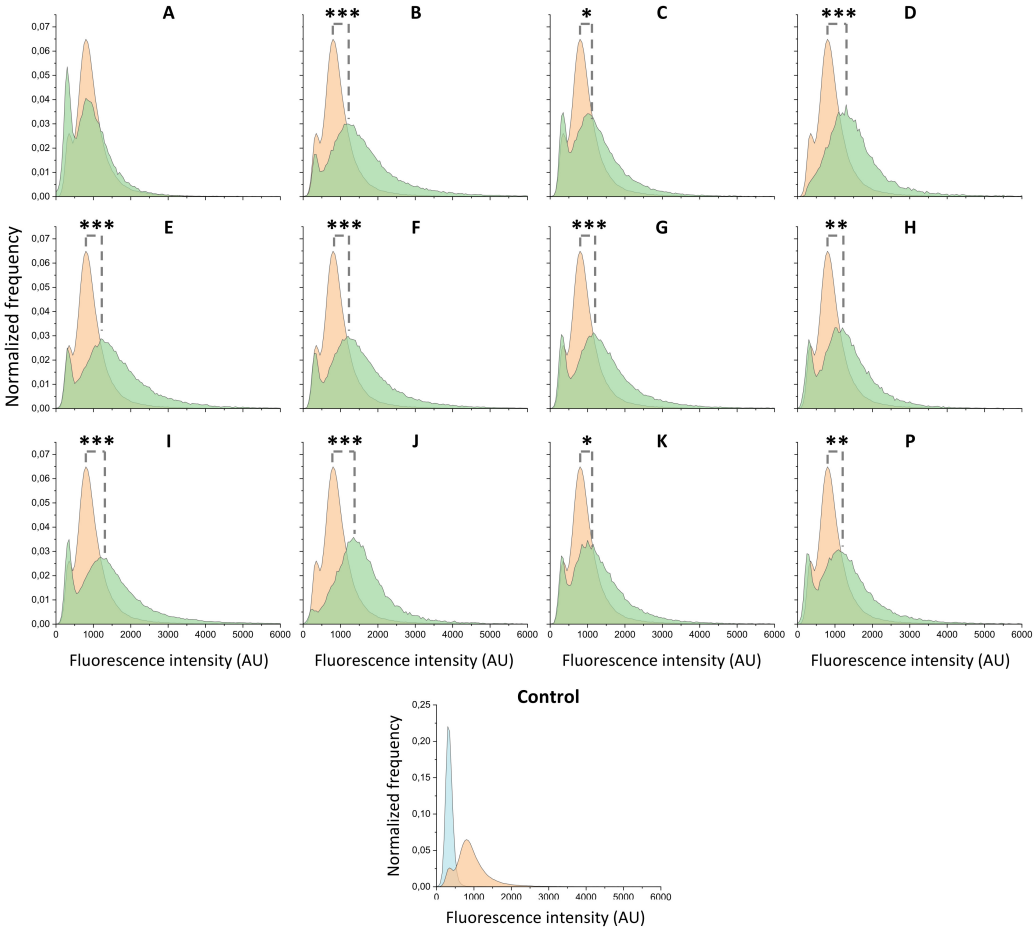

Fig. 1 Expression of the matrix gene *tapA* in *B. subtilis* WT and Δ*rap-phr* mutants after growth in MSgg under shaking conditions. Flow cytometry analysis showing the average distributions of GFP expression of Δ*rap-phr* mutants and WT harboring the P_{tapA}-*gfp* construct (n=3-8). The average WT distribution is shown in each graph for comparison. Orange = WT, green = mutant, blue = non-labelled control strain. Letters denotes the corresponding Δ*rap-phr* mutants, i.e. A = Δ*rapA*, B = Δ*rapB* and so forth. AU indicates arbitrary units. Significant difference in the mean fluorescence intensity of the ON population (GFP values between 500 and 10.000) between mutants and WT were tested by an ANOVA followed by Dunnett's Multiple Comparison test. *: P<0.05, **: P<0.01, ***: P<0.001.

Absence of certain Rap-Phr modules alters biofilm formation in vitro

Since matrix production is required for proper biofilm development (Branda *et al.*, 2006; Dragoš *et al.*, 2018), and most Δ*rap-phr* mutants showed increased matrix gene expression under shaking conditions in MSgg, we hypothesized that this would manifest in more complex and robust biofilm formation. To investigate this, WT and mutants were tested for their ability to form biofilm on a solid surface (MSgg agar) and robust pellicle biofilms at the MSgg medium-air interface. The pellicle forms as oxygen in the medium is exhausted and *B. subtilis* moves towards higher oxygen concentrations, thus the air-medium surface, where cells create a biofilm (Hölscher *et al.*, 2015).

In accordance to previous work, *B. subtilis* WT produced a wrinkled colony on solid surface, as well as a robust, wrinkled pellicle (Gallegos-Monterrosa *et al.*, 2016) (Fig. 2). While Δ*rapA, B, J* and *K* formed more wrinkled colonies*,* Δ*rapI* and *P* formed complex but very small colonies on MSgg agar compared to the WT. In contrast*,* Δ*rapC* formed a large, transparent colony with fewer wrinkles than WT. When testing for development of pellicle biofilms, the WT formed a densely wrinkled pellicle (Fig. 2). The Δ*rapA*, *C*, *I* and *P* mutants formed thin and/or non-homogenous pellicles, while the qualitative assessment revealed no mutants with more robust pellicles than WT. Lastly, the Δ*rapD*, *E*, *F, G*and *H* mutants formed comparable biofilms to the WT. These results show that despite most *Δrap-phr* mutants showing increased matrix gene expression compared to WT, this did not necessarily manifest in more complex colonies and robust pellicles.

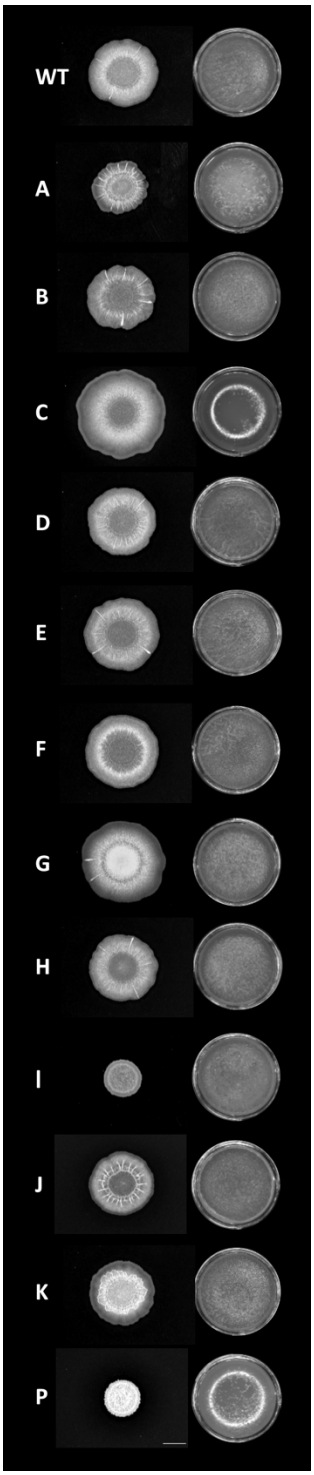

Fig. 2 Biofilm formation of *B. subtilis* WT and single Δ*rap-phr* mutants. ON cultures of *B. subtilis* WT and Δ*rap-phr* mutants were spotted on MSgg medium solidified with 1.5 % agar (left) or inoculated in MSgg with a starting OD_{600} = 0.05 (right). Images were taken from above after 48 h of incubation at 30°C using a stereomicroscope. Letters denote the corresponding Δ*rap* mutant, i.e. A = Δ*rapA*, B = Δ*rapB* and so forth. Bar denotes 5 mm for the biofilm colony images.

*Certain Δ*rap-phr *mutants are affected in colonization of* Arabidopsis thaliana *roots*

To reveal how the Rap-Phr modules affect biofilm formation in a more ecologically relevant environment, WT and mutants were tested for biofilm formation on the roots of the model plant organism *A. thaliana*. Previous studies have shown that matrix production is required for successful root colonization of *A. thaliana* (Beauregard *et al.*, 2013; Dragoš *et al.*, 2018). As with biofilms *in vitro*, we therefore speculated that the increased matrix gene expression observed in most strains would result in increased root colonization.

For this purpose, sterile *A. thaliana* seedlings with a root length of 0.5 to 1.2 cm were inoculated with one of the 12 Δ*rap-phr* mutants or WT and incubated in a plant chamber at 24°C (90 rpm) for 16 h, after which root colonization was quantified as colony forming unit (CFU) per mm root length. Of the 12 mutants tested, only Δ*rapD* and *P* mutants showed significantly increased root colonization compared to the WT (Fig. 3). In contrast, the *ΔrapI* mutant was significantly reduced in root colonization. The observation that Δ*rapI* and *P* showed similar biofilm formation *in vitro* (Fig. 2) but performed oppositely during root colonization (Fig. 3) might indicate that the effect of each individual Rap phosphatase on biofilm formation depends on the environment. Furthermore, similarly to biofilm formation *in vitro*, these results show that increased matrix production did not necessarily lead to increased root colonization.

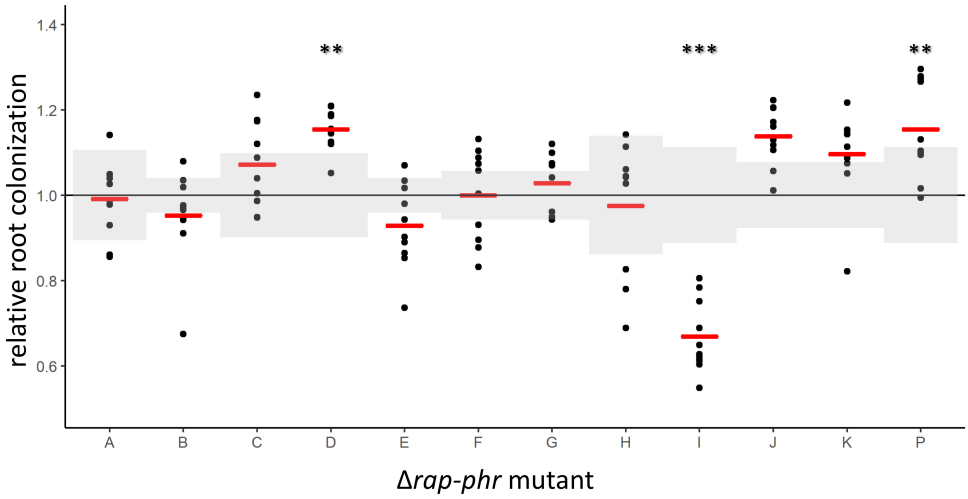

Fig. 3 *A. thaliana* root colonization by *B. subtilis* WT and single Δ*rap-phr* mutants. To estimate the impact of each of the Rap-Phr modules on root colonization, WT and single Δ*rap-phr* mutants were inoculated onto five-day-old seedlings of *A. thaliana* (n=7-10). After 16 h, CFU per mm root length was quantified. The log10-transformed value of CFU/mm root for each technical replicate was normalized to the mean of the WT from the same day. Each dot represents a root, while the mean value for each mutant is displayed as a red horizontal line. The black horizontal line represents the mean of the WT and the SD of the WT from each respective experiment is shown in shaded grey. For each assay, an ANOVA was performed on the log10-transformed values of CFU/mm root length. When significant (P<0.05), means were compared via Dunnett's multiple comparison test with WT as the control. When data failed to meet parametric assumptions, a Kruskal-Wallis test was performed followed by a Dunn's test. *: P<0.05, **: P<0.005, ***: P<0.001.

*Certain Δ*rap-phr *mutants show altered growth compared to WT*

The timing of biofilm initiation *in vitro* and on the root depends on the cell density, as at sufficiently high cell density the Phr peptides will only reach threshold concentrations allowing them to be imported into the cell, where they will inhibit their cognate Rap phosphatases, resulting in phosphorylation of Spo0A and expression of biofilm genes. Biofilm formation is therefore affected by growth rate, as strains growing faster will reach the threshold density for biofilm formation earlier. In order to test whether the observed changes in biofilm formation *in vitro* and on the root could be (partly) attributed to altered growth, the 12 Δ*rap-phr* mutants were tested for growth in MSgg under shaken conditions. For clear visualization, the growth curves of the 12 mutants were separated into four plots (Fig. 4). Of the 12 mutants tested, only Δ*rapA*, *I* and *P* showed altered growth profile compared to WT. Δ*rapA* and *I* showed a reduced growth rate, a delayed entry into stationary phase and reduced max OD_{590}. In addition, Δ*rapI* had a prolonged

stationary phase as well as slower decline during late stationary phase (possibly death phase). Δ*rapP* showed slower growth during exponential phase, about 10 h longer than the WT, but displayed a higher max OD_{590} at stationary phase. In LB medium, the same mutants were similarly or less affected in growth compared to WT (Fig. S1). The impaired growth of Δ*rapA* and *I* is in accordance with these two mutants forming thin and/or non-homogeneous pellicles (Fig.2), and Δ*rapI* displaying reduced root colonization (Fig. 3). In contrast, the prolonged exponential growth of Δ*rapP* is contradicting to the thin pellicle formed by this mutant, but correlating with the increased root colonization observed for this mutant. While the mutants have differential biofilm forming capacity *in vitro* and on the root; interestingly, this cannot be directly correlated with the growth rates of the mutants.

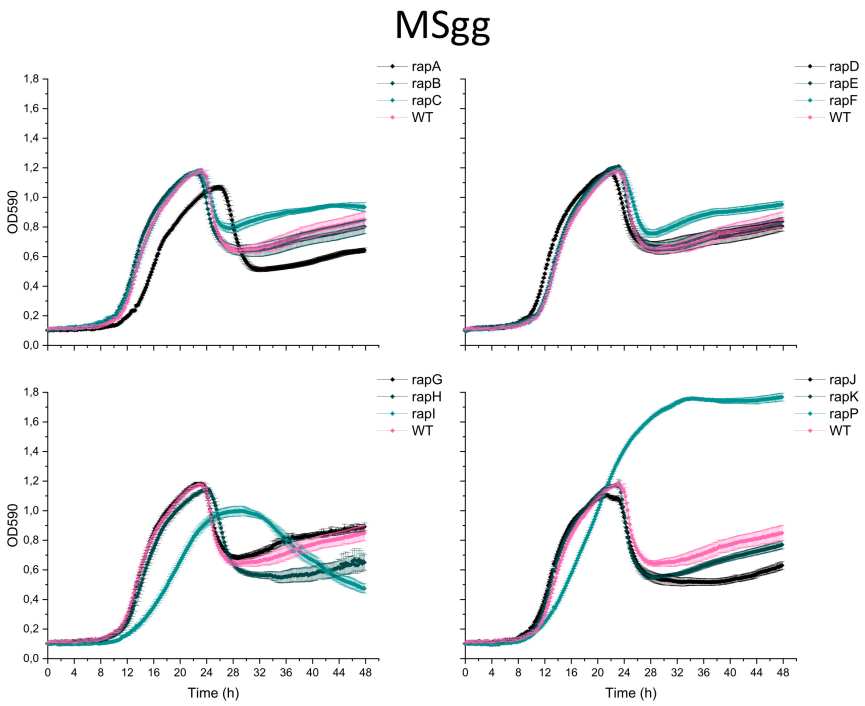

Fig. 4 Growth of *B. subtilis* WT and single Δ*rap-phr* mutants in MSgg. WT and mutants were inoculated into 96-well plates with a starting OD_{590} of 0.05. OD_{590} was measured every 10 min for 48 h at 30°C; each time point represents the mean of six technical replicates from two ON cultures (N=6). Error bars represent standard error (SE).

Discussion

For decades, the Rap-Phr regulatory systems which control the activity of the three master regulators governing cell differentiation in *B. subtilis* have been extensively studied (Pottahil and Lazazzera, 2003; Perego, 2013). However, since most studies have investigated the Rap-Phr networks independently from each other, in different genetic backgrounds and under distinct conditions, it is difficult to compare the results from these studies. Here, we investigated all 12 Rap-Phr systems found in *B. subtilis* 3610 for their role in matrix gene expression and biofilm development *in vitro*. In addition, we examined the role of Rap-Phr systems in colonization of plant roots for the first time.

Several of the Rap phosphatases have been reported to dephosphorylate Spo0F~P (Perego, 2013; Omer Bendori *et al.*, 2015) which is expected to influence matrix production, but only RapP has previously been demonstrated to affect matrix gene expression (Parashar, Konkol, *et al.*, 2013; Omer Bendori *et al.*, 2015). We were therefore interested in testing the effect of each of the 12 Rap-Phr systems on matrix gene expression. Inspired by a previously established method (Kearns *et al.*, 2005), expression from the promoter of the *tapA-sipW-tasA* operon was measured for WT and the 12 Δ*rap-phr* mutants in MSgg under shaking conditions. Only Δ*rapA* showed a significantly reduced relative ON population compared to the WT. Such reduced relative proportion of Δ*rapA* cells in the ON state may be due to more cells committing to activation of the sporulation pathway, and therefore attenuating induction of matrix genes (Bischofs *et al.*, 2009). Despite only some of the Rap phosphatases have been reported to dephosphorylate Spo0F~P (Perego, 2013; Omer Bendori *et al.*, 2015), we observed that all mutants except Δ*rapA* showed increased matrix gene expression. This indicates that despite the diversity in Rap-Phr systems, and the seeming redundancy of several Rap phosphatases regulating the same master regulator (Perego, 2013), each of the 12 Rap-Phr systems has a regulatory role that affects matrix gene expression under the tested conditions. The involvement of 12 Rap-Phr systems in influencing matrix gene expression suggests that the production of these costly public goods are under stringent control, and allows the

integration of multiple signals in order to fine-tune the timing and level of matrix production in response to different conditions (Auchtung *et al.*, 2006; Dragoš *et al.*, 2018).

Matrix production is well known to be required for biofilm formation under laboratory conditions (Branda *et al.,* 2006; Arnaouteli *et al.,* 2021). Moreover, matrix production and localized cell death have been shown to be responsible for the formation of wrinkles during biofilm development (Branda *et al.*, 2006; Asally *et al.*, 2012; Gallegos-Monterrosa *et al.*, 2017). We therefore speculated that the increased matrix production observed for all mutants, except Δ*rapA*, would manifest in these 11 mutants forming more wrinkled colonies as well as more robust pellicles compared to the WT. However, only some of the mutants were affected in biofilm formation. In accordance with increased matrix production, Δ*rapB, J* and *K* mutants formed more wrinkled colonies, and Δ*rapI* and *P* formed complex, though very small colonies compared to the WT. Moreover, Δ*rapC* formed a larger, smoother and more transparent colony. Furthermore, Δ*rapA,* with similar mean expression of the *tapA* operon and a smaller relative ON population compared to WT, also formed a more wrinkled colony. Surprisingly, pellicle robustness and complexity of the WT were not exceeded by any of the mutants. In contrast, Δ*rapA*, *C*, *I* and *P* formed thinner and/or non-homogenous pellicles. We thereby observed that the measured matrix gene expression not necessarily correlated with the formation of biofilms *in vitro*.

Next, we were interested in studying how Rap-Phr systems affect biofilm formation of *B. subtilis* in a more ecologically relevant environment, i.e. the plant root. Similarly to biofilm formation *in vitro*, biofilm formation on the plant root by *B. subtilis* depends on matrix gene expression regulated by Spo0A (Beauregard *et al.*, 2013; Chen *et al.*, 2013). We therefore hypothesized that the increased matrix production observed for most mutants would allow more bacterial cells to attach to and colonize the root. However, only Δ*rapD* and *P* showed increased root colonization, while Δ*rapI* was reduced in root colonization. The biofilm and root colonization experiments thereby show that the magnitude of matrix gene expression does not directly correlate with biofilm formation *in vitro* or on the root. Notably, matrix

gene expression was measured under heavily shaking conditions (220 rpm), while colonies and pellicles were developed under static conditions, and root colonization was performed under mildly shaken conditions (90 rpm). Such difference in conditions may affect matrix gene expression, and the mutants may not display the same increased matrix production under these conditions. Nonetheless, a lack of positive correlation between matrix gene expression and biofilm formation is in accordance with a previous study which showed that the magnitude of expression of *epsA-O* and *tasA-sipW-tasA* in *B. subtilis* 168 variants did not directly correlate with formation of wrinkled biofilms (Gallegos-Monterrosa *et al.*, 2016). These experiments thus support that biofilm formation *in vitro* as well as on plant roots is influenced by additional factors than just matrix gene expression. For example surfactin production, which is regulated by ComA – a target of several Rap phosphatases – was shown to influence the colony structure of *B. subtilis* 3610 on MSgg, though this secondary metabolite was not essential for pellicle formation and root colonization (Thérien *et al.*, 2020).

Interestingly, several studies have reported a correlation between the ability of strains to form robust biofilms and to colonize the root – both within and among strains (Chen *et al.*, 2013; Gallegos-Monterrosa *et al.*, 2016). However, the ability of the Δ*rap-phr* mutants to form biofilm *in vitro* did not necessarily reflect the ability to colonize the root (compare Fig. 2 and 3). For example, Δ*rapA* and *C* formed thin and non-homogenous pellicles but were able to colonize the root to similar levels as the WT. In addition, Δ*rapD* displayed comparable biofilm to the WT, but was significantly increased in root colonization. Finally, both Δ*rapI* and *P* showed reduced colony size and thin and/or non-homogenous pellicle formation, but while Δ*rapI* showed reduced root colonization, Δ*rapP* was increased in root colonization compared to the WT. In the study by Gallegos-Monterrosa *et al.* (2016), showing that strains forming robust pellicles also efficiently colonize the root, the *B. subtilis* 168 variants displayed genetic variation in various loci, resulting in large differences among the strains in their ability to form biofilm and colonize the root. In contrast,

the Δ*rap-phr* mutations studied here might only slightly modulate the regulatory pathways of *B. subtilis*, therefore the ability to form biofilm and colonize the root is less altered when compared to WT.

Nonetheless, the same study also demonstrated that biofilm development is influenced by medium composition (Gallegos-Monterrosa *et al.*, 2016). Besides static vs mild agitation and a temperature difference (30 vs 24°C), the media used for testing colony and pellicle formation, and for testing root colonization also slightly differ. First, the MSgg medium used for colony and pellicle formation contains a 10 times higher concentration of glycerol (0.5 %) compared to the MSNg medium used for plant root colonization (0.05 %). During plant root colonization, the bacteria thus depend on plant polysaccharides and root exudates as carbon source. In addition, *in vitro* biofilm development depends on the availability of iron and manganese (Kolodkin-Gal *et al.*, 2013; Shemesh and Chai, 2013; Mhatre *et al.*, 2016), while during plant root colonization in MSNg, biofilm formation is induced by plant polysaccharides (Beauregard *et al.*, 2013). The presence of plant polysaccharides may therefore allow mutants that form weak pellicle biofilms *in vitro* to efficiently colonize the root *(ΔrapA*, *C* and *P*, Fig. 2 and 3). Thereby, the pathways regulating matrix gene expression and other factors important for biofilm formation may be differently regulated under distinct conditions.

To conclude, we here show that all 12 Rap-Phr systems have an impact on matrix gene expression. Thereby, the diversity in Rap-Phr systems in *B. subtilis* could function to integrate multiple signals in order to fine-tune the timing and level of responses to new ecological niches, such as those it will encounter in soil. Furthermore, we demonstrated that matrix gene expression does not directly correlate with biofilm formation *in vitro* and on the root, and moreover that the ability to form biofilm *in vitro* not necessarily reflect the ability to colonize the root. These findings thus support that other components beyond matrix gene expression are important for biofilm establishment, and advocate that the pathways involved in matrix gene expression and these other components could be differently influenced under distinct conditions.

Experimental procedures

Bacterial strains and cultivation methods

Strains used in this study are listed in Table 1. The *B. subtilis* DK1042 strain (a natural competent derivative of the undomesticated NCBI 3610)(Konkol *et al.*, 2013) was used as WT. The 12 single Δ*rap-phr* mutants were previously created (Gallegos-Monterrosa *et al.*, 2020). For flow cytometry, the Δ*rap-phr* mutants were transformed with the plasmid phy_mKATE2 harboring the *mKATE* gene under the control of the hyper-spank constitutive promoter and a chloramphenicol (Chl) resistance gene within the flanking regions of the *amyE* gene (van Gestel *et al.*, 2014). Transformants were identified by selecting for Chl resistance, and double cross overs were verified by the loss of amylase activity. The resulting mKATE-labelled Δ*rap-phr* mutants were transformed with gDNA from *B. subtilis* TB373, which harbors the P_{tapA}-*gfp* reporter construct with a kanamycin (Km) resistance gene integrated at the *sacI* locus. Successful transformants with the reporter construct inserted into the *sacI* locus were identified by selecting for Km resistance. The resulting reporter strains were verified for reporter activity under the fluorescence stereomicroscope.

For all experiments, strains were grown over night in Lysogeny broth (LB; Lennox, Carl Roth; 10 $g \cdot l^{-1}$ tryptone, 5 $g \cdot l^{-1}$ yeast extract and 5 $g \cdot l^{-1}$ NaCl) at 37°C while shaking (220 rpm). When relevant, antibiotics were used at the following working concentrations: kanamycin (Km): 10 $\mu g \cdot l^{-1}$ and chloramphenicol (Chl): 5$\mu g \cdot l^{-1}$. For analyzing biofilm formation and matrix gene expression, strains were grown in MSgg (5 $mmol \cdot l^{-1}$ potassium phosphate [pH 7], 0.1 $mol \cdot l^{-1}$ 3-(N-morpholino)propanesulfonic acid (MOPS) [pH 7], 2 $mmol \cdot l^{-1}$ $MgCl_2$, 700 $\mu mol \cdot l^{-1}$ $CaCl_2$, 100 $\mu \cdot l^{-1}$ $MnCl_2$, 50 $\mu mol \cdot l^{-1}$ $FeCl_3$, 1 $\mu mol \cdot l^{-1}$ $ZnCl_2$, 2 $\mu mol \cdot l^{-1}$ thiamine, 0.5% glycerol, and 0.5% K-glutamate). For root colonization assay, strains were grown in MSNg (5 $mmol \cdot l^{-1}$ potassium phosphate buffer [pH 7], 0.1 $mol \cdot l^{-1}$ MOPS [pH 7], 2 $mmol \cdot l^{-1}$ $MgCl_2$, 50 $\mu mol \cdot l^{-1}$ $MnCl_2$, 1$\mu mol \cdot l^{-1}$ $ZnCl_2$, 2 $\mu mol \cdot l^{-1}$ thiamine, 700 $\mu mol \cdot l^{-1}$ $CaCl_2$, 0.2 % NH_4Cl_2, and 0.05 % glycerol).

Microscopy imaging

All images were acquired with an Axio Zoom V16 stereomicroscope (Carl Zeiss, Germany) equipped with a Zeiss CL 9000 LED light source and an AxioCam MRm monochrome camera (Carl Zeiss, Germany).

Biofilm formation assay

For biofilm formation on a solid surface, 7 µL ON cultures were spotted on MSgg supplemented with 1.5 % agar. For pellicle biofilm formation at the liquid-air interface, 15 µl inoculum of ON cultures adjusted to OD_{600} of 5 was added to 1.5 ml MSgg medium, giving a starting OD_{600} of 0.05. Plates were incubated under static conditions at 30°C for 48 h, thereafter images of the arisen colonies and pellicles were obtained using the stereomicroscope.

Root colonization assay

A. thaliana Col-0 plants were used as a host for *B. subtilis* root colonization. *A. thaliana* seeds were sterilized in 2% (v/v) sodium hypochlorite (NaOCl) for 10 minutes with an orbital shaker. Following this, NaOCl was removed and the seeds were washed five times in sterile water. Sterilized seeds were placed in MS agar plates (Murashige and Skoog basal salts, Sigma) (2.2 $g \cdot l^{-1}$) with approximately 20 seeds per petri dish. The petri dishes were wrapped in parafilm and left for stratification at 4°C for 3 days, and were then moved to the plant chamber (cycles of 16 h light at 24°C and 8 h dark at 20°C). After five to seven days, seedlings of 0.5-1.2 cm in size were placed in 48-well plates containing 270 µl MSNg medium per well. To each well, 30 µl of ON culture adjusted to OD_{600} of 0.2 was added resulting in a final starting OD_{600} of 0.02. The plates were sealed with parafilm and incubated in the plant chamber while shaking at 90 rpm for 16 h. Seedlings were then washed in MSNg to remove non-attached cells from the root. The washed seedlings were placed in Eppendorf tubes containing 1mL of NaCl (0.9 %) and subjected to standard sonication protocol to disperse the biofilm (Dragoš *et al.*, 2018). The resulting bacterial cell suspension was diluted

and plated on LB agar plates for CFU counting. To acquire the CFU per mm root the obtained CFU was divided by the length of the corresponding root.

Growth profiling

To follow the growth of WT and mutants, two ON cultures of each strain were independently inoculated into a 96-well plate containing MSgg or LB broth, at a starting OD_{590} and OD_{600}, respectively, of 0.05. Growth was monitored in a plate reader (Infinite F200 PRO, TECAN and BioTek Synergy HTX Multi-Mode Microplate Reader) every 10 min for 48 h at 30°C.

Matrix gene expression assays by flow cytometry

To measure expression from the matrix operon *tapA-sipW-tasA*, mKate-labelled WT and Δ*rap-phr* mutants harboring the reporter construct P_{tapA}-*gfp* were incubated in 10 ml MSgg in 100 ml blue cap bottles with a starting OD_{600} of 0.02. Lids were loosely on, so oxygen would not be depleted. Bottles were incubated at 37°C at 220 rpm for 6 h. After incubation, 1 ml of each sample was transferred to a 2 ml Eppendorf tube and samples were run on the flow cytometer (MACSQuant® VYB, Miltenyibiotec). mKate-positive cells were detected by yellow laser (561 nm) and filter Y3 (661/20 nm). Green fluorescent cells, representing the cells expressing the *tapA-sipW-tasA* operon, were detected by the blue laser (488 nm) and filter B1 (525/50 nm). Strain TB35 with constitutive mKate expression was used as a negative control for GFP expression, while strain TB34 with constitutive GFP expression was used as a positive control for GFP expression. In addition, TB34 and a medium control were used to identify the red background fluorescence noise due to autofluorescence, and cells above this background fluorescence were identified as the mKate positive cells representing *B. subtilis* cells producing the mKate protein. For each WT and mutant sample, single events were identified on the SSC-H vs SSC-A plot and gated into the mKate-A vs SSC-A plot, where mKate positive cells were identified. These gated cells were exported and read into

Excel where the green fluorescence (GFP-A) values were used for analysis. To get rid of negative values, 300 was added to all events in the samples. To obtain the distribution of GFP expression, data obtained from each replicate was subjected to binning with identical bin size (of 50). Events with GFP expression from 0 to 10.000 were included as the majority of events were within this interval (>98 %). Next, the number of events in each bin was divided by the total number of events in the given replicate, resulting in the normalized frequency. To obtain the mean distribution, a mean frequency for each bin was obtained by averaging the individual frequencies within this bin across the replicates, resulting in the mean distribution of single-cell-level expression. For statistics, the relative OFF (GFP values between 0 and 500) and ON (GFP values between 500-10.000) populations were calculated for each replicate, as was the mean fluorescence of the ON population.

Statistical analysis

Statistical analyses were performed in R Studio. For each root colonization assay, a one-way analysis of variance (ANOVA) was performed on the log10-transformed data. When adjusted P-values were significant ($P<0.05$), a Dunnett's Multiple Comparison test was performed. When data failed to meet parametric assumptions (normality and equal variance), a non-parametric analysis (Kruskal-Wallist test) was used. If adjusted P-values were significant ($P<0.05$), treatment means were compared via a Dunn test. To test for significant differences in relative OFF/ON population and mean fluorescence of ON population between mutants and WT, an ANOVA followed by Dunnett's Multiple Comparison test was performed. Significance level for all tests were set at 5 %.

Acknowledgements

We thank Mikael Lenz Strube for his suggestions on statistics. The work was supported by a DTU Bioengineering start-up fund to ÁTK. Funding from Novo Nordisk Foundation (grant NNFOC0055625) for the infrastructure "Imaging microbial language in biocontrol (IMLiB)" is acknowledged.

Authors' contributions: M.N.C. and Á.T.K. conceived the project; M.N.C., R.M.R.M., N.K.K. performed experiments; R.G.-M. created mutant strains; M.N.C. analyzed the data; M.N.C. and Á.T.K. wrote the manuscript with feedback from all authors.

Conflict of interests

The authors declare that there is no conflict of interests in relation to the work described.

Table 1: Strains used in this study

Name	Description	Reference
DK1042	NCIB 3610 *coml*^{Q12I}	(Konkol *et al.*, 2013)
TB499	DK1042 *rapA*::Km^{R}	(Gallegos-Monterrosa *et al.*, 2020)
TB575	DK1042 Δ*rapB*	(Gallegos-Monterrosa *et al.*, 2020)
TB396	DK1042 Δ*rapC*:: Km^{R}	(Gallegos-Monterrosa *et al.*, 2020)
TB315	DK1042 Δ*rapD*:: Km^{R}	(Gallegos-Monterrosa *et al.*, 2020)
TB339	DK1042 Δ*rapE*::Spec^{R}	(Gallegos-Monterrosa *et al.*, 2020)
TB341	DK1042 Δ*rapF*::Spec^{R}	(Gallegos-Monterrosa *et al.*, 2020)
TB404	DK1042 Δ*rapG*::Spec^{R}	(Gallegos-Monterrosa *et al.*, 2020)
TB405	DK1042 Δ*rapH*::Spec^{R}	(Gallegos-Monterrosa *et al.*, 2020)
TB272	DK1042 Δ*rapI*::Km^{R}	(Gallegos-Monterrosa *et al.*, 2020)
TB274	DK1042 Δ*rapJ*::Km^{R}	(Gallegos-Monterrosa *et al.*, 2020)
TB557	DK1042 Δ*rapK*::Km^{R}	(Gallegos-Monterrosa *et al.*, 2020)
TB435	DK1042 Δ*rapP*::Mls^{R}	(Gallegos-Monterrosa *et al.*, 2020)
TB588	DK1042 Δ*rapA*	(Gallegos-Monterrosa *et al.*, 2020)
TB410.1	DK1042 Δ*rapC*	(Gallegos-Monterrosa *et al.*, 2020)
TB513	DK1042 Δ*rapD*	(Gallegos-Monterrosa *et al.*, 2020)
TB444	DK1042 Δ*rapI*	(Gallegos-Monterrosa *et al.*, 2020)
TB411.2	DK1042 Δ*rapJ*	(Gallegos-Monterrosa *et al.*, 2020)
TB587	DK1042 Δ*rapK*	(Gallegos-Monterrosa *et al.*, 2020)
DTUB189	DK1042 Δ*rapA*, *amyE*::$P_{hyspank}$-*mKATE* Chl^{R}	This study
DTUB165	DK1042 Δ*rapB*, *amyE*::$P_{hyspank}$-*mKATE* Chl^{R}	This study
DTUB190	DK1042 Δ*rapC*, *amyE*::$P_{hyspank}$-*mKATE* Chl^{R}	This study
DTUB191	DK1042 Δ*rapD*, *amyE*::$P_{hyspank}$-*mKATE* Chl^{R}	This study
DTUB159	DK1042 Δ*rapE*::Spec^{R}, *amyE*::$P_{hyspank}$-*mKATE* Chl^{R}	This study
DTUB160	DK1042 Δ*rapF*::Spec^{R}, *amyE*::$P_{hyspank}$-*mKATE* Chl^{R}	This study
DTUB166	DK1042 Δ*rapG*::Spec^{R}, *amyE*::$P_{hyspank}$-*mKATE* Chl^{R}	This study

DTUB167	DK1042 Δ*rapH*::Spec^R, *amyE*::P$_{hyspank}$-*mKATE* Chl^R	This study
DTUB192	DK1042 Δ*rapI*, *amyE*::P$_{hyspank}$-*mKATE* Chl^R	This study
DTUB193	DK1042 Δ*rapJ*, *amyE*::P$_{hyspank}$-*mKATE* Chl^R	This study
DTUB194	DK1042 Δ*rapK*, *amyE*::P$_{hyspank}$-*mKATE* Chl^R	This study
DTUB173	DK1042 Δ*rapP*::Mls^R, *amyE*::P$_{hyspank}$-*mKATE* Chl^R	This study
TB34	DK1042 *amyE*::P$_{hyspank}$-*gfp* Chl^R	(Mhatre *et al.*, 2017)
TB35	DK1042 *amyE*::P$_{hyspank}$-*mKATE* Chl^R	(Hölscher *et al.*, 2016)
TB865	DK1042 *amyE*::P$_{hyspank}$-*mKATE* Chl^R, *sacA*::P$_{tapA}$-*gfp* Km^R	(Dragoš *et al.*, 2018)
DTUB284	DK1042 Δ*rapA amyE*::P$_{hyspank}$-*mKATE* Chl^R, *sacA*::P$_{tapA}$-*gfp* Km^R	This study
DTUB285	DK1042 Δ*rapB, amyE*::P$_{hyspank}$-*mKATE* Chl^R, *sacA*::P$_{tapA}$-*gfp* Km^R	This study
DTUB286	DK1042 Δ*rapC*, *amyE*::P$_{hyspank}$-*mKATE* Chl^R, *sacA*::P$_{tapA}$-*gfp* Km^R	This study
DTUB287	DK1042 Δ*rapD*, *amyE*::P$_{hyspank}$-*mKATE* Chl^R, *sacA*::P$_{tapA}$-*gfp* Km^R	This study
DTUB288	DK1042 Δ*rapE*::Spec^R, *amyE*::P$_{hyspank}$-*mKATE* Chl^R, *sacA*::P$_{tapA}$-*gfp* Km^R	This study
DTUB289	DK1042 Δ*rapF*::Spec^R, *amyE*::P$_{hyspank}$-*mKATE* Chl^R, *sacA*::P$_{tapA}$-*gfp* Km^R	This study
DTUB290	DK1042 Δ*rapG*::Spec^R, *amyE*::P$_{hyspank}$-*mKATE* Chl^R, *sacA*::P$_{tapA}$-*gfp* Km^R	This study
DTUB291	DK1042 Δ*rapH*::Spec^R, *amyE*::P$_{hyspank}$-*mKATE* Chl^R, *sacA*::P$_{tapA}$-*gfp* Km^R	This study
DTUB292	DK1042 Δ*rapI*, *amyE*::P$_{hyspank}$-*mKATE* Chl^R, *sacA*::P$_{tapA}$-*gfp* Km^R	This study
DTUB293	DK1042 Δ*rapJ*, *amyE*::P$_{hyspank}$-*mKATE* Chl^R, *sacA*::P$_{tapA}$-*gfp* Km^R	This study
DTUB294	DK1042 Δ*rapK*, *amyE*::P$_{hyspank}$-*mKATE* Chl^R, *sacA*::P$_{tapA}$-*gfp* Km^R	This study
DTUB295	DK1042 Δ*rapP*::Mls^R, *amyE*::P$_{hyspank}$-*mKATE* Chl^R, *sacA*::P$_{tapA}$-*gfp* Km^R	This study
TB373	DK1042 *sacA*::P$_{tapA}$-*gfp* Km^R	(Gallegos-Monterrosa *et al.*, 2016)

References

Asally, M., Kittisopikul, M., Rué, P., Du, Y., Hu, Z., Çağatay, T., *et al*. (2012) Localized cell death focuses mechanical forces during 3D patterning in a biofilm. *Proc Natl Acad Sci U S A* **109**: 18891–18896.

Arnaouteli, S., Bamford, N., Stanley-Wall, N., and Kovács, Á. T. (2021) *Bacillus subtilis* biofilm formation and social interactions. *Nat Rev Microbiol*

Auchtung, J.M., Lee, C.A., and Grossman, A.D. (2006) Modulation of the ComA-dependent quorum response in *Bacillus subtilis* by multiple Rap proteins and Phr peptides. *J Bacteriol* **188**: 5273–5285.

Bais, H.P., Fall, R., and Vivanco, J.M. (2004) Biocontrol of *Bacillus subtilis* against infection of *Arabidopsis* roots by *Pseudomonas syringae* is facilitated by biofilm formation and surfactin production. *Plant Physiol* **134**: 307–319.

Beauregard, P.B., Chai, Y., Vlamakis, H., Losick, R., and Kolter, R. (2013) *Bacillus subtilis* biofilm induction by plant polysaccharides. *Proc Natl Acad Sci U S A* **110**: 1621–1630.

Belas, R. (2013) When the swimming gets tough, the tough form a biofilm. *Mol Microbiol* **90**: 1–5.

Bischofs, I.B., Hug, J.A., Liu, A.W., Wolf, D.M., and Arkin, A.P. (2009) Complexity in bacterial cell-cell communication: quorum signal integration and subpopulation signaling in the *Bacillus subtilis* phosphorelay. *Proc Natl Acad Sci U S A* **106**: 6459–6464.

Blake, C., Christensen, M.N., and Kovács, Á.T. (2021) Molecular aspects of plant growth promotion and protection by *Bacillus subtilis*. *Mol Plant Microbe Interact* **34**: 15–25.

Bongiorni, C., Ishikawa, S., Stephenson, S., Ogasawara, N., and Perego, M. (2005) Synergistic regulation of competence development in *Bacillus subtilis* by two Rap-Phr systems. *J Bacteriol* **187**: 4353–4361.

Branda, S.S., Chu, F., Kearns, D.B., Losick, R., and Kolter, R. (2006) A major protein component of the *Bacillus subtilis* biofilm matrix. *Mol Microbiol* **59**: 1229–1238.

Branda, S.S., González-Pastor, J.E., Ben-Yehuda, S., Losick, R., and Kolter, R. (2001) Fruiting body

formation by *Bacillus subtilis*. *Proc Natl Acad Sci U S A* **98**: 11621–11626.

Cairns, L.S., Hobley, L., and Stanley-Wall, N.R. (2014) Biofilm formation by *Bacillus subtilis*: new insights into regulatory strategies and assembly mechanisms. *Mol Microbiol* **93**: 587–598.

Cairns, L.S., Marlow, V.L., Bissett, E., Ostrowski, A., and Stanley-Wall, N.R. (2013) A mechanical signal transmitted by the flagellum controls signalling in *Bacillus subtilis*. *Mol Microbiol* **90**: 6–21.

Chen, Y., Cao, S., Chai, Y., Clardy, J., Kolter, R., Guo, J.H., and Losick, R. (2012) A *Bacillus subtilis* sensor kinase involved in triggering biofilm formation on the roots of tomato plants. *Mol Microbiol* **85**: 418–430.

Chen, Y., Yan, F., Chai, Y., Liu, H., Kolter, R., Losick, R., and Guo, J.H. (2013) Biocontrol of tomato wilt disease by *Bacillus subtilis* isolates from natural environments depends on conserved genes mediating biofilm formation. *Environ Microbiol* **15**: 848–864.

Comella, N. and Grossman, A.D. (2005) Conservation of genes and processes controlled by the quorum response in bacteria: characterization of genes controlled by the quorum-sensing transcription factor ComA in *Bacillus subtilis*. *Mol Microbiol* **57**: 1159–1174.

Core, L. and Perego, M. (2003) TPR-mediated interaction of RapC with ComA inhibits response regulator-DNA binding for competence development in *Bacillus subtilis*. *Mol Microbiol* **49**: 1509–1522.

Costerton, J.W., Lewandowski, Z., DeBeer, D., Caldwell, D., Korber, D., and James, G. (1994) Biofilms, the customized microniche. *J Bacteriol* **176**: 2137–2142.

Dragoš, A., Kiesewalter, H., Martin, M., Hsu, C.Y., Hartmann, R., Wechsler, T., et al. (2018) Division of labor during biofilm matrix production. *Curr Biol* **28**: 1903-1913.

Even-Tov, E., Omer Bendori, S., Pollak, S., and Eldar, A. (2016) Transient duplication-dependent divergence and horizontal transfer underlie the evolutionary dynamics of bacterial cell-cell signaling. *PLoS Biol* **14**: e2000330.

Fall, R., Kinsinger, R.F., and Wheeler, K.A. (2004) A simple method to isolate biofilm-forming *Bacillus*

subtilis and related species from plant roots. *Syst Appl Microbiol* **27**: 372–379.

Flemming, H.C. and Wingender, J. (2010) The biofilm matrix. *Nat Rev Microbiol* **8**: 623–633.

Fujita, M., González-Pastor, J.E., and Losick, R. (2005) High- and low-threshold genes in the Spo0A regulon of *Bacillus subtilis*. *J Bacteriol* **187**: 1357–1368.

Gallegos-Monterrosa, R., Christensen, M.N., Barchewitz, T., Köppenhöfer, S., Priyadarshini, B., Bálint, B., et al. (2020) Impact of Rap-Phr system abundance on adaptation of *Bacillus subtilis*. *bioRxiv* 2020.09.01.278184.

Gallegos-Monterrosa, R., Kankel, S., Götze, S., Barnett, R., Stallforth, P., and Kovács, Á.T. (2017) *Lysinibacillus fusiformis* M5 induces increased complexity in *Bacillus subtilis* 168 colony biofilms via hypoxanthine. *J Bacteriol* **199**: e00204-17.

Gallegos-Monterrosa, R., Mhatre, E., and Kovács, Á.T. (2016) Specific *Bacillus subtilis* 168 variants form biofilms on nutrient-rich medium. *Microbiol* **162**: 1922–1932.

Van Gestel, J., Weissing, F. J., Kuipers, O. P. & Kovács, A.T. (2014) Density of founder cells affects spatial pattern formation and cooperation in *Bacillus subtilis* biofilms. *ISME J* **8**: 2069–2079.

Hall-Stoodley, L., Costerton, J.W., and Stoodley, P. (2004) Bacterial biofilms: from the natural environment to infectious diseases. *Nat Rev Microbiol* **2**: 95–108.

Hölscher, T., Bartels, B., Lin, Y.C., Gallegos-Monterrosa, R., Price-Whelan, A., Kolter, R., *et al*. (2015) Motility, chemotaxis and aerotaxis contribute to competitiveness during bacterial pellicle biofilm development. *J Mol Biol* **427**: 3695–3708.

Hölscher, T., Dragoš, A., Gallegos-Monterrosa, R., Martin, M., Mhatre, E., Richter, A., and Kovács, Á.T. (2016) Monitoring spatial segregation in surface colonizing microbial populations. *J Vis Exp* **116**: e54752.

Jiang, M., Shao, W., Perego, M., and Hoch, J.A. (2000) Multiple histidine kinases regulate entry into stationary phase and sporulation in *Bacillus subtilis*. *Mol Microbiol* **38**: 535–542.

Kearns, D.B., Chu, F., Branda, S.S., Kolter, R., and Losick, R. (2005) A master regulator for biofilm formation by *Bacillus subtilis*. *Mol Microbiol* **55**: 739–749.

Kiesewalter, H.T., Lozano-Andrade, C.N., Wibowo, M., Strube, M.L., Maróti, G., Snyder, D., et al. (2021) Genomic and chemical diversity of *Bacillus subtilis* secondary metabolites against plant pathogenic fungi. *mSystems* **6**: e00770-20.

Kolodkin-Gal, I., Elsholz, A.K.W., Muth, C., Girguis, P.R., Kolter, R., and Losick, R. (2013) Respiration control of multicellularity in *Bacillus subtilis* by a complex of the cytochrome chain with a membrane-embedded histidine kinase. *Genes Dev* **27**: 887–899.

Konkol, M.A., Blair, K.M., and Kearns, D.B. (2013) Plasmid-encoded ComI inhibits competence in the ancestral 3610 strain of *Bacillus subtilis*. *J Bacteriol* **195**: 4085–4093.

López, D. and Kolter, R. (2010) Extracellular signals that define distinct and coexisting cell fates in *Bacillus subtilis*. *FEMS Microbiol Rev* **34**: 134–149.

Lopez, D., Vlamakis, H., and Kolter, R. (2009) Generation of multiple cell types in *Bacillus subtilis*. *FEMS Microbiol Rev* **33**: 152–163.

López, D., Vlamakis, H., and Kolter, R. (2010) Biofilms. *Cold Spring Harb Perspect Biol* **2**: a000398.

McLoon, A.L., Guttenplan, S.B., Kearns, D.B., Kolter, R., and Losick, R. (2011) Tracing the domestication of a biofilm-forming bacterium. *J Bacteriol* **193**: 2027–2034.

Mhatre, E., Monterrosa, R.G., and Kovács, Á.T. (2014) From environmental signals to regulators: modulation of biofilm development in Gram-positive bacteria. *J Basic Microbiol* **54**: 616–632.

Mhatre, E., Sundaram, A., Hölscher, T., Mühlstädt, M., Bossert, J., and Kovács, Á.T. (2017) Presence of calcium lowers the expansion of *Bacillus subtilis* colony biofilms. *Microorganisms* **5**: 7.

Mhatre, E., Troszok, A., Gallegos-Monterrosa, R., Hölscher, T., Kuipers, O.P., Lindst, S., and Kovács, Á.T. (2016) The impact of manganese on biofilm development of *Bacillus subtilis*. *Microbiology* **162**: 1468–1478.

O'Toole, G., Kaplan, H.B., and Kolter, R. (2000) Biofilm formation as microbial development. *Annu Rev Microbiol* **54**: 49–79.

Ogura, M. and Fujita, Y. (2007) *Bacillus subtilis* RapD, a direct target of transcription repression by RghR, negatively regulates *srfA* expression. *FEMS Microbiol Lett* **268**: 73–80.

Omer Bendori, S., Pollak, S., Hizi, D., and Eldar, A. (2015) The RapP-PhrP quorum-sensing system of *Bacillus subtilis* strain NCIB3610 affects biofilm formation through multiple targets, due to an atypical signal-insensitive allele of RapP. *J Bacteriol* **197**: 592–602.

Ongena, M. and Jacques, P. (2008) *Bacillus* lipopeptides: versatile weapons for plant disease biocontrol. *Trends Microbiol* **16**: 115–125.

Parashar, V., Jeffrey, P.D., and Neiditch, M.B. (2013) Conformational change-induced repeat domain expansion regulates Rap phosphatase quorum-sensing signal receptors. *PLoS Biol* **11**: e1001512.

Parashar, V., Konkol, M.A., Kearns, D.B., and Neiditch, M.B. (2013) A plasmid-encoded phosphatase regulates *Bacillus subtilis* biofilm architecture, sporulation, and genetic competence. *J Bacteriol* **195**: 2437–2448.

Perego, M. (2013) Forty years in the making: understanding the molecular mechanism of peptide regulation in bacterial development. *PLoS Biol* **11**: e1001516.

Perego, M., Glaser, P., and Hoch, J.A. (1996) Aspartyl-phosphate phosphatases deactivate the response regulator components of the sporulation signal transduction system in *Bacillus subtilis*. *Mol Microbiol* **19**: 1151–1157.

Perego, M. and Hoch, J.A. (1996) Cell-cell communication regulates the effects of protein aspartate phosphatases on the phosphorelay controlling development in *Bacillus subtilis*. *Proc Natl Acad Sci U S A* **93**: 1549–1553.

Piggot, P.J. and Hilbert, D.W. (2004) Sporulation of *Bacillus subtilis*. *Curr Opin Microbiol* **7**: 579–586.

Di Pippo, F., Di Gregorio, L., Congestri, R., Tandoi, V., and Rossetti, S. (2018) Biofilm growth and control

in cooling water industrial systems. *FEMS Microbiol Ecol* **94**: fiy044.

Pottahil, M. and Lazazzera, B. A. (2003) The extracellular Phr peptide-Rap phosphatase signaling circuit of *Bacillus subtilis. Front Biosci* **8**: 32–45.

Reizer, J., Reizer, A., Perego, M., and Saier, M.H. (1997) Characterization of a family of bacterial response regulator aspartyl-phosphate (RAP) phosphatases. *Microb Comp Genomics* **2**: 103–111.

Shemesh, M. and Chai, Y. (2013) A combination of glycerol and manganese promotes biofilm formation in *Bacillus subtilis* via histidine kinase KinD signaling. *J Bacteriology* **195**: 2747–2754.

Singh, R., Paul, D., and Jain, R.K. (2006) Biofilms: implications in bioremediation. *Trends Microbiol* **14**: 389–397.

Stewart, P.S. (2002) Mechanisms of antibiotic resistance in bacterial biofilms. *Int J Med Microbiol* **292**: 107–113.

Thérien, M., Kiesewalter, H.T., Auria, E., Charron-Lamoureux, V., Wibowo, M., Maróti, G., et al. (2020) Surfactin production is not essential for pellicle and root-associated biofilm development of *Bacillus subtilis*. *Biofilm* **2**: 100021.

Verhamme, D.T., Kiley, T.B., and Stanley-Wall, N.R. (2007) DegU co-ordinates multicellular behaviour exhibited by *Bacillus subtilis*. *Mol Microbiol* **65**: 554–568.